

Landscape-scale variation in forest structure and biomass along an elevation gradient in the Atlantic Forest of the Serra do Mar, Brazil

Veronika Leitold¹
Michael Keller^{2,3}
Douglas C Morton⁴
Yosio E Shimabukuro¹

¹ Instituto Nacional de Pesquisas Espaciais - INPE
São José dos Campos - SP, 12227-010 Brasil
{vleitold, yosio}@dsr.inpe.br

² USDA Forest Service, International Institute of Tropical Forestry
San Juan, Puerto Rico, 00926 USA
mkeller.co2@gmail.com

³ EMBRAPA Monitoramento por Satélite
Campinas - SP, 13070-115 Brasil

⁴ NASA Goddard Space Flight Center
Greenbelt, MD, 20771 USA
douglas.morton@nasa.gov

Abstract. Landscape-scale quantification of forest structure, disturbance patterns and biomass distribution can improve our understanding of the environmental controls on the functioning of forested ecosystems. Assessing the detailed structure of the complex tropical forest canopy is a challenging task, especially in areas of steep topography where field access is limited. We used airborne lidar (light detection and ranging) data to describe the landscape-scale variation in canopy structure and gap distribution in a 1000-ha area along an elevation gradient from 0 to 1200m in the Atlantic Forest of the *Serra do Mar* in southeast Brazil. Mean canopy heights (MCHs) were greatest (21-22m) at intermediate elevations (200-700m) in the submontane forest where terrain slope was also the steepest (~40°). Canopy gap fraction was highest (~30%) and MCH lowest (~16m) in the montane forest areas (900-1100m) on flatter sites atop the plateau (~24° slopes). We used forest inventory data from nine 1-ha permanent field plots (PFPs) within the study area to assess aboveground biomass (AGB) stocks and changes. We established regression models based on lidar-derived canopy structure and field-based biometry data, and used these to extrapolate AGB predictions across the landscape. Comparing canopy height and disturbance distributions in the PFPs with the distributions across the broader landscape, we found that submontane PFPs showed closer correspondence with their surrounding areas, while montane PFPs consistently overestimated landscape-scale canopy height (thus AGB pools) and underestimated gap fraction (therefore AGB changes).

Keywords: airborne lidar, tropical montane forest, canopy structure, gap distribution, biomass dynamics, permanent field plots.

1. Introduction

Tropical forest structure and composition exhibit characteristic changes along elevation gradients, including declines in forest height, tree species diversity and live aboveground biomass (AGB) as elevation increases (GIRARDIN et al., 2013). In addition to the effects of altitude, the topography of the underlying substrate can also influence species composition and vegetation structure by providing microhabitat heterogeneity (CLARK et al., 1999). Understanding how environmental factors affect ecosystem processes in tropical forests is fundamental to predicting how these forests might respond to changes in land-use and global

climatic conditions. Additionally, characterization of tropical forest structure and biomass distribution is critical for a better understanding of the role of these ecosystems in the global carbon cycle.

Detailed information on the three-dimensional structure and function of tropical montane forests is particularly difficult to obtain and remains limited today (ASNER et al., 2014). Many studies have used field-based observations to assess vegetation structure and functional properties in forest plots. However, such inventories are often hindered by difficult access to remote sites and the limited spatial extent of measurements ($\leq 1\text{ha}$). Lidar remote sensing captures forest structure in great detail, and airborne lidar platforms allow for measurement of large-scale variability in forest structure. Structural metrics such as canopy height, sub-canopy topography, and the vertical distribution of canopies from lidar data can be used to model biophysically important attributes such as basal area, mean stem diameter and aboveground biomass (LEFSKY et al., 2002).

In this study, we analyzed lidar data from a 1000-ha montane forest area in the Brazilian Atlantic Forest of the *Serra do Mar* to describe the landscape-scale variation in canopy structure and gap distribution. We used forest inventory data from 1-ha permanent field plots (PFPs) to assess AGB stocks and changes and extrapolate biomass predictions across the landscape based on regression models between lidar-derived canopy structural parameters and field-based biometry data. Additionally, we evaluated the representativeness of the 1-ha PFPs of landscape-scale patterns in Atlantic Forest structure and biomass. Through the detailed characterization of forest structure and disturbance across the *Serra do Mar* landscape, this work contributes to our understanding of ecosystem processes in the coastal Atlantic Forest remnants beyond the scale of PFP measurements.

2. Material and methods

2.1 Study area

This study was carried out in an area of the São Paulo State Park of *Serra do Mar* (PESM) in southeast Brazil ($23^{\circ}17' - 23^{\circ}34'S$ and $45^{\circ}02' - 45^{\circ}11'W$), along an elevation gradient between 0 - 1200 m above sea level (a.s.l.). The topographically complex landscape of the *Serra do Mar* is covered by the dense vegetation of the Atlantic Forest, subdivided into vegetation types by elevation: lowland, submontane and montane forests from sea level to the mountain top. Mean annual rainfall in the area is approximately 2500 mm (JOLY et al., 2012), and monthly average temperatures vary by terrain elevation between $17.6^{\circ}\text{C} - 24.7^{\circ}\text{C}$ (SCARANELLO et al., 2012). Soils across the lowland, submontane and montane forest sites are classified as sandy-loam *Inceptisols* (ALVES et al., 2010).

2.2 Lidar data

Lidar data were collected in April 2012 over a rectangular strip of the PESM covering a total forest area of approximately 1000 ha ($1.5 \text{ km} \times 7 \text{ km}$). The Optech ALTM 3100 laser scanner instrument was operated at an average flying altitude of 1600 m a.s.l. Average pulse density was 12 m^{-2} (first/last mode) resulting in a mean return density of 20 m^{-2} across the landscape. Flight line data were consolidated into a unified point cloud by the commercial vendor (GEOID Ltda.), and further processing followed the G-LiHT methodology (COOK et al., 2013). The data products used in this study included the digital terrain model (DTM) and canopy height model (CHM) raster surfaces from G-LiHT processing at 1-m spatial resolution.

2.3 Field data

This study used data from nine PFPs that belong to a 14-plot network, established in 2006/07 to evaluate variation in forest diversity and ecosystem function along an altitudinal transect in the *Serra do Mar* (ALVES et al., 2010; JOLY et al., 2012). Out of the nine plots considered here, one is located in the lowland forest at 100 m elevation (Plot F), four plots in the submontane forest between 190 - 370 m (Plots G, H, I, J) and four plots in the montane forest at about 1000 m elevation (Plots K, L, M, N). Each plot is square-shaped with a projected area of 1 ha.

Live AGB stocks and changes were assessed using inventory data from the two most recent surveys in 2008/09 and 2011/12 (the latter census coinciding with the lidar data collection). To estimate biomass of trees, we applied Chave's et al. (2005) pan-tropical biomass allometry: $AGB_{tree} = 0.0509 \times \rho \times DBH^2 \times H$, where ρ is species-level wood density ($g\ cm^{-3}$), DBH is tree diameter at breast height (cm), and H is total tree height (m) estimated from stand-specific allometric equations (SCARANELLO et al., 2012). Live AGB estimates for palms were calculated using the allometric equation developed by Hughes (1997, cited in ALVES et al., 2010): $AGB_{palm} = \{\exp[0.9285 \ln(DBH^2) + 5.7236] \times 1.050001\} \div 10^3$. Tree ferns were not considered in the present study. Estimated components of AGB dynamics over the 3.5-year time period included: (i) AGB gain from growth and recruitment; (ii) AGB loss to mortality; and (iii) AGB net change (growth + recruitment – mortality), all expressed in the units $Mg\ ha^{-1}\ year^{-1}$.

2.4 Analyses

Lidar data were associated with the PFP locations based on ground control points measured with survey grade GNSS receivers at the corner markers of each square plot. The lidar-derived canopy height distribution of each PFP was described and compared to that of the surrounding landscape. The study area was divided into elevation classes in 100-m intervals, and canopy height distributions were generated for each elevation class (i.e.: 0-100 m, 100-200 m, 200-300 m, etc.). From the 1-m DTM raster, we extracted statistics related to terrain elevation and slope in the PFPs and across the broader landscape.

Canopy gap sizes and frequencies within PFPs were quantified using two gap definitions (similar to that of BROKAW, 1982): (i) gaps to 14 m above ground with a contiguous area of at least $10\ m^2$ ("mid-canopy gaps"), and (ii) gaps to 5 m above ground with a minimum area of $1\ m^2$ ("low-canopy gaps"). The maximum gap height thresholds tested for this optimization ranged from 1 m to 20 m in 1-meter increments, while the minimum gap area cutoff values tested were 1, 5, 10, 25, 50 and $100\ m^2$.

Regression models were developed between field-based biomass data and lidar-derived canopy height and gap fractions at the plot scale. Separate models were developed to characterize AGB, gap fraction, and AGB dynamics (gain, loss, and net change). These relationships were used to extrapolate the results to the entire study area at 1-ha spatial resolution.

3. Results and discussion

3.1 Canopy structure

Mean canopy heights (MCHs) in the 1-ha field plots were between 19.6 m to 22.9 m, while MCH at the landscape-scale varied between 15.7 m and 21.7 m (Figure 3.1). Canopy height distributions in the submontane forest plots (F–J) showed strong correspondence with

the surrounding landscape (< 1.5 m difference in MCH), while the montane plots had consistently larger MCHs than the surrounding area (+ 3.8 - 5.0 m difference). At the landscape scale, MCH values were largest in the submontane forests between ~ 200 - 700 m elevation (about 21.5 m MCH), where the terrain was also the steepest (~40° slopes). These results could indicate that steeper slopes favor tree growth or protection from human and natural disturbances. Indeed, the lowest MCH values were observed in the lowland forest below 100 m elevation (13.8 m MCH; consistent with a history of logging in this area) and also in the montane forest region between 900 - 1100 m a.s.l. (15.7 m MCH). The montane forest included several patches with very low MCH (Figure 3.1). Visual analysis of the DTM and hillshade images indicated flatter terrain (<15° slope) in these patches compared to the surrounding landscape, suggesting that poor soil drainage or inundation may influence vegetation structure and composition in these areas.

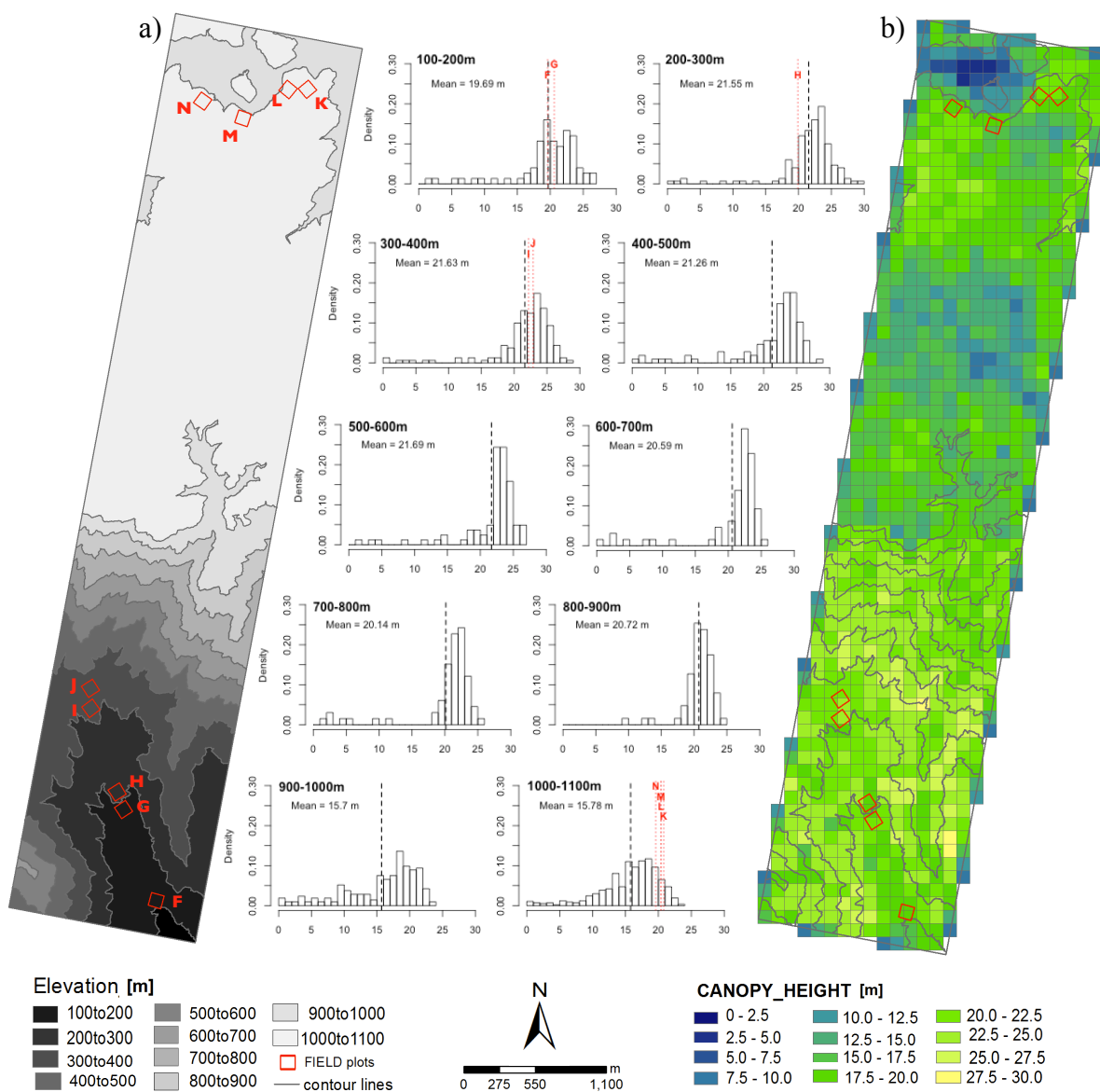


Figure 3.1 Elevation map of the study area (a), showing the location of PFPs, and the distribution of lidar-derived canopy heights at 1-ha resolution across the study area (b). Histograms show the distribution of MCH for each elevation class in (a), and vertical red

lines indicate the MCH for submontane Plots F–J and montane Plots K–N within their respective elevation classes.

3.2 Gap distribution

The range of *low-canopy* gap fractions across the nine permanent field plots was 0.04 - 1.71% (mean of 0.54%), while landscape-scale averages showed generally larger values: 1.22% across submontane forests and 3.25% in the montane forest region. Similarly, the range of *mid-canopy* gap fractions was much smaller in the field plots (2.17 - 12.86% with a mean of 7.98%) than across the surrounding landscape (7.94% in the submontane and 29.9% in montane forest areas). Mean and maximum gap sizes were also significantly larger on the landscape scale than in the 1-ha PFPs.

When comparing the submontane and montane forests, more gaps were found in the montane region, and those gaps were also larger in size. Both *low-canopy* and *mid-canopy* gap fractions were notably higher in the montane landscape than in the submontane landscape, yet the gap distributions within the PFPs (submontane and montane) did not reflect this difference. Soils and topography are potential explanations for the observed difference in gap distributions across the landscape; poorly-drained soils on more exposed montane forest sites may increase the risk of windthrow, while south-facing slopes and valleys may protect the submontane forests from wind damage.

3.3 Aboveground biomass

Total live aboveground biomass in PFPs ranged from 219.8 to 348.6 Mg ha⁻¹ across the nine locations based on the 2011/12 census (Table 3.1). Overall, net biomass change between 2008/09-2011/12 was small and negative in Plots G, H and N, close to zero in Plot M, and positive in Plots F, I, J, K and L. Mean annual AGB gain ranged from a low of 3.9 Mg ha⁻¹ y⁻¹ (Plot M) to a high of 5.7 Mg ha⁻¹ y⁻¹ (Plot F); on average, submontane plots showed higher rates of biomass gain (5.1 ± 0.6 Mg ha⁻¹ y⁻¹) than montane plots (4.3 ± 0.6 Mg ha⁻¹ y⁻¹). Calculated rates of mortality were more variable across the nine plots, ranging from a minimum loss of 1.8 Mg ha⁻¹ y⁻¹ (Plot J) to a maximum of 5.7 Mg ha⁻¹ y⁻¹ (Plot N).

Table 3.1 Components of aboveground biomass (2011/12) and dynamics (between 2008/09 and 2011/12) in the nine permanent field plots F–N.

COMPONENTS OF BIOMASS	Submontane plots					Montane plots					mean \pm stdev
	F	G	H	I	J	K	L	M	N		
Total AGB T1 (Mg ha⁻¹)	214.2	289.5	268.4	308.5	328.1	281.7 \pm 43.8	326.5	268.4	348.5	276.3	304.9 \pm 38.8
Total AGB T2 (Mg ha⁻¹)	219.8	286.5	267.1	319.9	338.7	286.4 \pm 46.5	332.5	270.5	348.6	274.5	306.5 \pm 39.9
AGB GAIN (Mg ha⁻¹ y⁻¹)	5.7	4.2	5.2	5.5	4.6	5.1 \pm 0.6	4.4	4.0	3.9	5.1	4.3 \pm 0.5
AGB LOSS (Mg ha⁻¹ y⁻¹)	4.4	5.0	5.5	2.4	1.8	3.8 \pm 1.6	2.4	3.3	3.8	5.7	3.8 \pm 1.4
NET Change (Mg ha⁻¹ y⁻¹)	1.3	-0.7	-0.3	3.1	2.7	1.2 \pm 1.7	2.0	0.7	0.0	-0.6	0.5 \pm 1.1
Survey interval (years)	4.2	4.1	4.1	3.7	3.9	4.0	3.0	3.0	2.1	2.9	3.4

3.4 Lidar-biomass relationships

Mean canopy height (MCH) predicted 43% of the variation in total AGB in the permanent field plots (RMSE = 30.0 Mg ha⁻¹, p-value = 0.054), with a positive relationship between these two variables: AGB = 24.13 × MCH - 204.76. Using this model, we extrapolated

biomass predictions to the whole study area at 1-ha resolution (Figure 3.1.b). Landscape-scale AGB predictions averaged into elevation classes ranged from a minimum of 193.3 Mg ha⁻¹ in the montane forest (1000 - 1100 m a.s.l) to a maximum of 337.1 Mg ha⁻¹ between 400 - 500 m elevation within the submontane forest area (Figure 3.2.a). The mean predicted AGB across the montane landscape (196.7 Mg ha⁻¹) was significantly lower than the average AGB calculated from the four montane PFPs (306.5 Mg ha⁻¹). In comparison, the mean AGB value across the submontane landscape was notably higher (324.5 Mg ha⁻¹) than the average of the five submontane PFPs (286.4 Mg ha⁻¹).

Components of aboveground biomass dynamics estimated from field inventory data over a 3.5-year period proved to be strong predictors of canopy gap fraction in the 1-ha plots. Mid-canopy gap fraction was very strongly related to net AGB change in the 1-ha plots ($R^2 = 0.91$, p-value < 0.001), and mortality rates were also significantly related to mid-canopy gap fraction across the nine PFPs ($R^2 = 0.87$, p-value < 0.001). Variation in biomass gain was not strongly correlated with gap fraction (*low-canopy* definition; $R^2 = 0.1$, p-value = 0.42), however, removing one point from the analysis (Plot N with unusually high gap fraction compared to other plots) greatly improved this relationship ($R^2 = 0.76$, p-value < 0.005).

Landscape-scale distributions of mid and low-canopy gap fractions (MCG% and LCG%, respectively) were sampled onto 1-ha raster grids, which were then used to predict components of biomass dynamics (in Mg ha⁻¹ year⁻¹) across the landscape using three separate equations: (i) AGB Net Change = $-0.365 \times MCG\% + 3.822$; (ii) AGB Loss = $0.352 \times MCG\% + 1.012$; (iii) AGB Gain = $-1.992 \times LCG\% + 5.464$. The whole-area maps of the resulting landscape-scale distributions are shown in Figure 3.2 (b, c and d) and the terrain, canopy height and predicted biomass statistics are summarized in Table 3.2.

Table 3.2 Lidar-derived terrain and canopy metrics and predicted AGB stocks (2011/12) and dynamics (between 2008/09 and 2011/12) across the elevation range of the study area.

AVERAGE METRICS BY ELEVATION CLASS	Elevation Intervals [m]										
	0-100	100-200	200-300	300-400	400-500	500-600	600-700	700-800	800-900	900-1000	1000-1100
Surface Area (ha)	4.2	46.5	88.8	94.2	51.7	38.9	29.0	31.8	30.5	106.1	470.7
Terrain Slope (°)	16.0	26.2	31.7	34.7	40.4	40.9	41.0	40.7	41.6	25.8	22.5
Canopy Height (m)	17.34	20.67	22.91	22.73	23.40	23.05	22.66	21.94	21.58	16.59	16.94
Mid-canopy Gaps (%)	28.4	12.9	7.8	6.5	6.9	6.1	6.4	8.2	10.6	35.7	28.6
Low-canopy Gaps (%)	4.1	2.1	1.2	0.9	1.3	1.3	0.9	0.9	1.3	7.9	2.2
Predicted AGB (Mg ha⁻¹)	231.1	290.7	332.4	335.9	337.1	334.6	325.6	313.1	294.2	211.9	193.3
AGB LOSS (Mg ha⁻¹ y⁻¹)	7.8	5.2	3.8	3.5	3.7	3.3	3.4	3.8	4.8	7.0	7.6
AGB GAIN (Mg ha⁻¹ y⁻¹)	0.8	1.6	3.3	3.5	2.3	2.7	3.2	3.5	2.9	2.4	2.8
NET Change (Mg ha⁻¹ y⁻¹)	-3.2	-0.5	0.9	1.2	1.1	1.4	1.3	0.9	-0.1	-2.4	-3.0

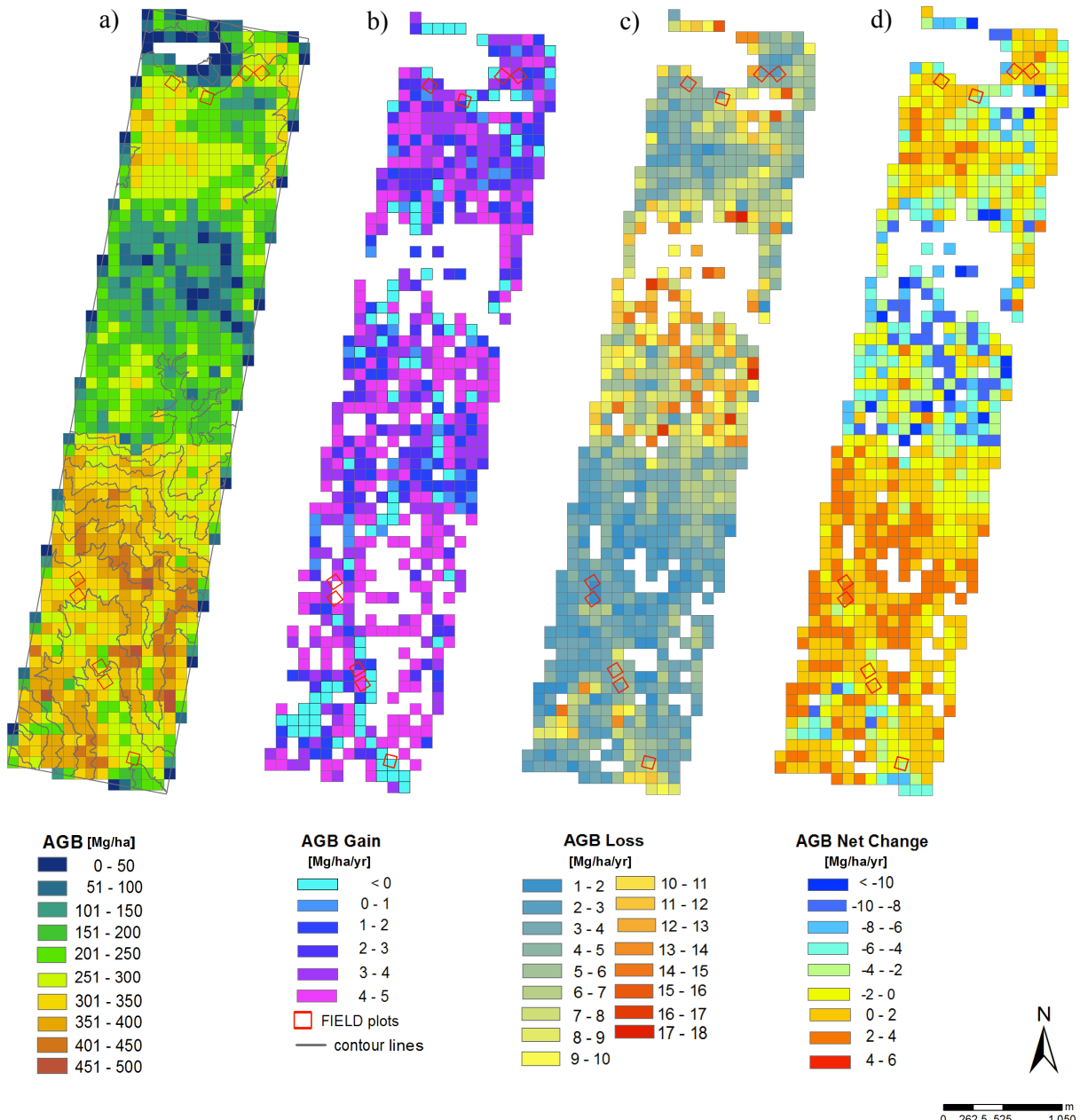


Figure 3.2 Landscape patterns of modeled (a) total AGB stocks (Mg ha^{-1}), (b) AGB Gain, (c) AGB Loss and (d) AGB Net Change ($\text{Mg ha}^{-1} \text{y}^{-1}$) at 1-ha spatial resolution.

4. Conclusions

Five main conclusions can be drawn from the analysis of lidar and PFP data at the *Serra do Mar* site:

- [1] The nine permanent field plots within our study area did not provide a faithful representation of the landscape-scale variability of canopy heights, gap fraction and aboveground biomass, as they failed to capture the extremes of these distributions.
- [2] The integration of lidar observations with field measurements might be improved by employing an alternative approach, wherein the study area is overflowed with lidar first, and the derived data products (e.g. terrain, MCH, gaps) are used to optimize sampling in the field.
- [3] Mean canopy height was a good predictor of aboveground biomass in the 1-ha permanent

plots, and this predictive relationship might be improved with multivariate regression techniques making use of additional lidar-derived metrics.

[4] Processes of aboveground biomass dynamics, principally mortality and net change, were reflected in the lidar-derived distribution of static canopy gaps, suggesting that lidar-based estimates of forest structure reflects the memory of recent forest disturbances.

[5] Future studies with multi-temporal lidar would allow for the direct examination of gap dynamics and canopy height changes, further elucidating the processes of biomass gain through growth and recruitment.

Acknowledgements

This research was supported by NASA's Terrestrial Ecology and Carbon Monitoring System Programs (NASA NNH13AW64I) and scholarship from CAPES. Lidar data were acquired with support from USAID, the US Department of State, EMBRAPA and the US Forest Service Office of International Programs. Forest inventory work was supported by USAID and FAPESP (03/12595-7 to C. A. Joly and L. A. Martinelli), within the BIOTA/FAPESP Program (COTEC/IF 41.065/2005, COTEC/IF 663/2012 and IBAMA/CGEN 093/2005 permits). We thank Luciana F. Alves for sharing the biomass data of the Atlantic forest sites.

References

- ALVES, L. F.; VIEIRA, S. A.; SCARANELLO, M. A.; CAMARGO, P. B.; SANTOS, F. A. M.; JOLY, C. A.; MARTINELLI, L. A. Forest structure and live aboveground biomass variation along an elevational gradient of tropical Atlantic moist forest (Brazil). **Forest Ecology and Management**, v. 260, p. 679-691, 2010.
- ASNER, G. P.; ANDERSON, C. B.; MARTIN, R. E.; KNAPP, D. E.; TUPAYACHI, R.; SINCA F.; MALHI, Y. Landscape-scale changes in forest structure and functional traits along an Andes-to-Amazon elevation gradient. **Biogeosciences**, v. 11, p. 843-856, 2014.
- BROKAW, N. V. The definition of treefall gap and its effect on measures of forest dynamics. **Biotropica**, v. 14, p. 158-160, 1982.
- CHAVE, J.; ANDALO, C.; BROWN, S.; CAIRNS, M. A.; CHAMBERS, J. Q.; EAMUS, D.; FOLSTER, H. et al. Tree allometry and improved estimation of carbon stocks and balance in tropical forests. **Oecologia**, v. 145, n. 1, p. 87-99, 2005.
- CLARK, D. B.; PALMER M. W.; CLARK, D. A. Edaphic factors and the landscape-scale distributions of tropical rain forest trees. **Journal of Ecology**, v. 80, p. 2662-2675, 1999.
- COOK, B. D.; CORP, L. A.; NELSON, R. F.; MIDDLETON, E. M.; MORTON, D. C.; MCCORKEL, J. T.; MASEK, J. G.; RANSON, K. J.; LY, V.; MONTESANO, P. M. NASA Goddard's LiDAR, Hyperspectral and Thermal (G-LiHT) Airborne Imager. **Remote Sensing**, v. 5, p. 4045-4066, 2013.
- GIRARDIN, C. A. J.; FARFAN-RIOS, W.; GARCIA, K.; FEELEY, K. J.; JØRGENSEN, P. M.; MURAKAMI, A. A.; PÉREZ, L. C. et al. Spatial patterns of above-ground structure, biomass and composition in a network of six Andean elevation transects. **Plant Ecology & Diversity**, DOI: 10.1080/17550874.2013.820806, 2013.
- JOLY, C. A.; ASSIS, M. A.; BERNACCI, L. C.; TAMASHIRO, J. Y.; CAMPOS, M. C. R.; GOMES, J. A. M. A. et al. Floristic and phytosociology in permanent plots of the Atlantic Rainforest along an altitudinal gradient in southeastern Brazil. **Biota Neotropica**, v. 12, p. 125-145, 2012.
- LEFSKY, M. A.; COHEN, W. B.; PARKER, G. G.; HARDING, D. J. Lidar remote sensing for ecosystem studies. **BioScience**, v. 52, n. 1, p. 19-30, 2002.
- SCARANELLO, M. A. S.; ALVES, L. F.; VIEIRA, S. A.; CAMARGO, P. B.; JOLY, C. A.; MARTINELLI, L. A. Height-diameter relationships of tropical Atlantic moist forest trees in southeastern Brazil. **Scientia Agricola**, v. 69, p. 26-37, 2012.